FLEXIBILITY OF 'CLAY MATS'

D.C.Wijeyesekera, E.W.K.Loh
Built Environment Research Group
d.c.wijeyesekera@uel.ac.uk; ericwkloh@uel.ac.uk

Abstract: This paper presents a scientific development to addressing the current absence of a convenient technique to identify the ductile to brittle transition of clay mats. The applicability of clay mats can be brought into question if they become brittle due to drying in hot weather / tropical climates. Bentonite clay mats produced with different liquid polymers and at different moisture content were used in the study. The dependence of flexural stiffness on moisture content is presented. All the specimens showed that the flexibility of the clay mat declined exponentially with decreasing moisture content. Often one would adopt the feeling from a finger pressure test to give a perception of the softness / stiffness of the material. The paper also presents an extension of this concept to adopt an appropriately modified Brinell hardness test for the clay mats. Concurrently, 3 point bending tests were carried out on samples of the clay mat to obtain a value for the elastic structural stiffness (EI). The paper further confirms a strong correlation between Brinell Hardness Test and the structural stiffness. This study helps to assess the performance of clay mats with different proportions of additives that have been introduced in the mat manufacture to delay the inevitable drying characteristics of the mat, when exposed to hostile thermal environments.

1. Introduction:

Clays rolled into the form of a mat have been used as facial masks by beauticians in the cosmetic industry and as skin care / pain relief products in the pharmaceutical industry. As of recent times, larger bentonite clay mats are used in the form of composite contaminant barriers or as structural waterproofing in the construction industry. In order to meet the potential to be an effective contaminant barrier in hostile geochemical environments, a factory controlled prehydration with cation exchange resisting polymer prior to installation is always necessary (McLoughlin, 2004., Wijeyesekera, 2003).

The factory manufacturing process requires the clays to be at an appropriate moisture condition to facilitate the rolling process and also possess sufficient flexibility and tensile strength to remain integral. These clays are essentially fine grained and it is critical that the consistency of the clay is preserved to ensure that the mat remains flexible with no possibility of it developing brittle fractures. However, if the clay mat dries, the flexibility can reduce to the point where it can become brittle.

The quality control measure for the clay mats could be improved significantly if the understanding of ductile to brittle transition with regard to flexibility of the clay mat was addressed. Research in this area, however, in comparison with other aspects of engineering behaviour of clay, has been minimal despite its obvious significance as a basic physical characteristic of clay. One could argue that this critical moisture content is near the plastic limit of the clay. In this note, the present paper will describe the new testing approach to quantify the flexibility of clay mat and discussed the influence of isothermally drying of the clay mat on its flexibility and attempts to establish the workable limits of moisture contents for the mats.

2. Materials and Methods:

2.1. Samples Properties:

Two sets of clay mats, namely PA and PB were used in the experimental measurements. PA and PB were formed with the addition of distinctively different liquid polymer A and B, and vacuum extruded to a thickness of 5 mm. One of the primary purposes of the liquid polymer treatment is to improve the mechanical properties of the clay mats.
All specimens were cut with a razor blade to the required dimensions as described in each test. These samples were initially kept in the oven at 40°C for various time intervals to achieve the desired equilibrium moisture content. The isothermal drying kinetic of the specimens have been described elsewhere (Wijeyesekera and Loh, 2005). The drying rate of PB is reduced with the appropriate addition of a new polymer. Discussion in the new polymer is beyond the remit of this paper.

2.2. Flexural Stiffness Measurement:

The principal observations comprised of load-deformation curves for all the specimens where simply supported to produce transverse bending. A modified version of the standard 3-point bend test, ASTM D790 (see Figure 1) was used to quantify structural stiffness, *EI* (where *E* is the Modulus of Elasticity and *I* is the area moment of inertia). The 3-point bending was chosen over alternatives such as 4-point or cantilever bending to prevent excess plastic deformation at the load point and failure under self-weight. With this procedure, a rectangaloid specimen (cross-section a×b) was flexed across a small load point to provide the mid-span deflection. The sample dimensions (120×50×5mm) were selected by a length/thickness and width/thickness ratio of 24 and 10 as recommended by Mylvaganam, 2006.
At the onset of testing, the specimen is balanced against self-weight on two supports. To avoid excessive plastic deformation, an increment of 20g at each time was applied. The mid-span deflection of the specimens was observed through the movable optical measurement system.
Flexural stiffness, *EI* can be calculated by the following equation:

$$EI = \frac{WL^3}{48\Delta} \qquad (1)$$

where *EI* is the flexural stiffness [Nm^2], *W* is the load [N], *L* is the specimen length between two support point [m] and Δ is the mid-span deflection.
Typical load-deflection graphs of the specimens are shown in Figures 3 and 4. It can be seen that as the moisture content of the samples is decreased, the curve becomes more linear, i.e., the variation of slope with mid-span deflection becomes smaller, and the samples become less ductile. Slope, *m* of the initial linear portion of the graph is used in the evaluation of *EI* as shown in Equation 2.

$$EI = \frac{mL^3}{48} \qquad (2)$$

where *EI* is the flexural stiffness [Nm^2], *m* is the initial slope of the load vs. deflection curve and *L* is the specimen length between two support point [m]

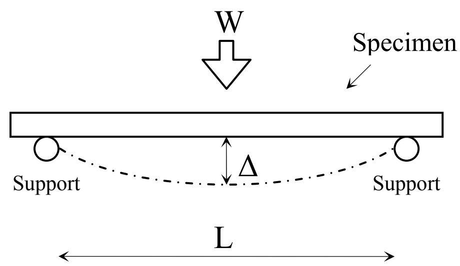

Figure 1 Schematic diagram of the standard 3-point bend test

2.3. Brinell Hardness Test:

The Brinell hardness test is widely used in industrial metallurgy. The test observes the indentation made on the specimens by forcing a hard steel sphere of a specified diameter under a specified load into the surface of a material and measuring the diameter of the indentation left after the test. The Brinell hardness number (BHN) is expressed as the load F divided by the surface area of the indentation (Dieter, 1988). A well structured Brinell hardness number reveals the test conditions, and is presented like this "75 HB 10/500/30". This means that a Brinell Hardness of 75 was obtained using a 10mm diameter hardened steel sphere with a 500 kilogram load applied for a period of 30 seconds. This is expressed by the following formula:

$$BHN = \frac{F}{\frac{\pi}{2} D \times \left(D - \sqrt{D^2 - D_i^2} \right)} \quad (3)$$

where *BHN* is the Brinell hardness number [the result is equivalent to pressure measurement, but the units are rarely stated], *F* is the imposed load [N], *D* is the diameter of the spherical indenter [mm] and D_i is the diameter of the resulting indenter impression [mm]. To overcome the difficulties encountered during measuring the size of the residual imprint, a continuous indentation test approach was adopted as an alternative to the conventional way.

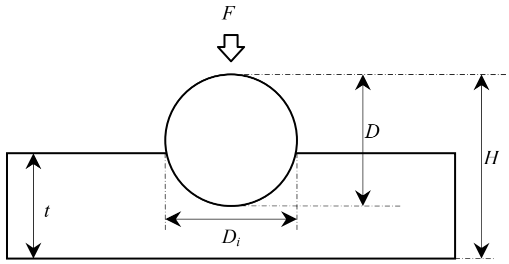

Figure 2 Schematic diagram of Brinell hardness test

In the continuous indentation test, the indentation load-depth curve was obtained by continuously measuring the applied load and the penetration depth during the test. From the indentation load-depth curve, values for the final indenter diameter, D_i, can easily be obtained from the geometrical relationship as shown in Figure 2 and can be calculate from the following equation:

$$D_i = 2\sqrt{\left(\frac{D}{2}\right)^2 - \left(H - t - \frac{D}{2}\right)^2} \quad (4)$$

The continuous indentation testing was carried out on each 50-mm diameter samples, using a standard tri-axial apparatus with a spherical steel indenter of radius 6.35mm. The optimum diameter for the use of BHN measurement in clay liner was developed by Mylvaganam, 2006.

3. Results and Discussion:

The load-deflection behaviour of the specimen PA and PB with the moisture contents ranged from 10% to 40% are shown in Figure 3 and 4 respectively. The initial slope of each curve was markedly linear for all moisture content (10%-40%). However this was more pronounced in specimens with moisture content below

20%. Excessive plastic deformation was also observed as the governing mode of failure for the specimens with moisture content greater than 25%.

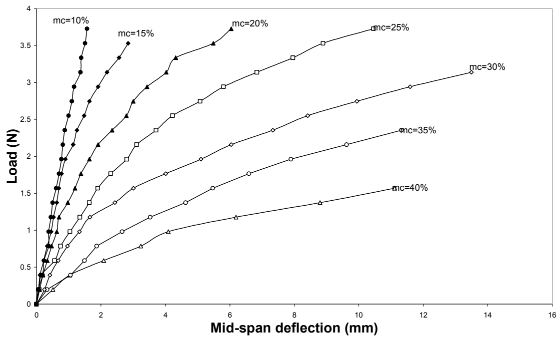

Figure 3 Test result of the load-deflection behaviour of the specimen PA

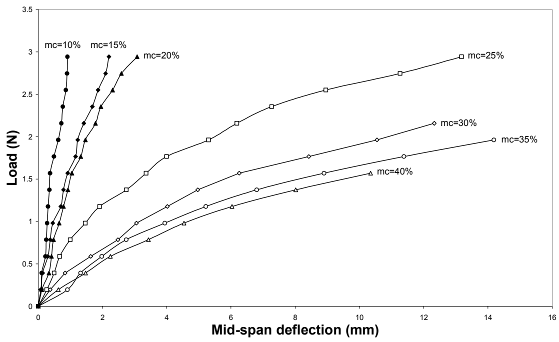

Figure 4 Test result of the load-deflection behaviour of the specimen PB

Moisture content variation effects on the flexural stiffness is investigated using a simplex exponential mathematical model and is presented in Figure 5.

Although the difference in the magnitudes of flexural stiffness between specimen PA and PB was not significant, but the ductile to brittle transition due to the moisture reduction in the specimens was apparent. As predicted, a decrease in moisture content will increase the stiffness of specimens and thus reduce the flexibility of the clay mats.

The specimens at different moisture contents were investigated for cracking on flexure. It may be observed that the critical stiffness, at which the specimens lose their malleability, occurs at moisture contents below 12%.

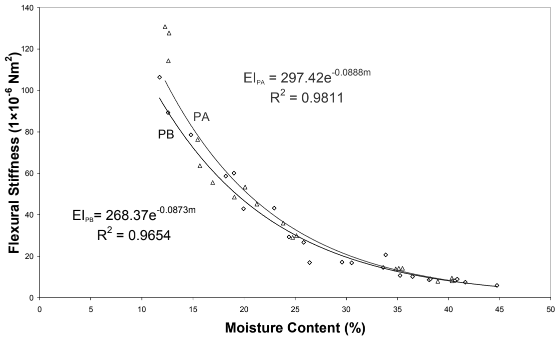

Figure 5 Flexural stiffness of specimen PA and PB

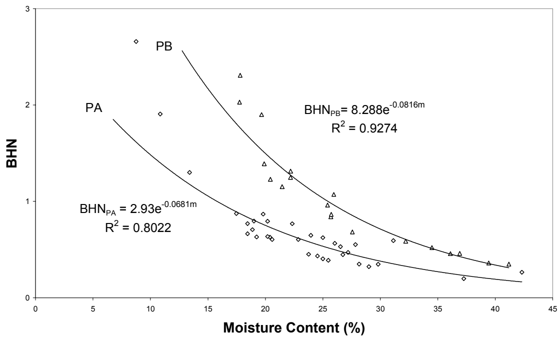

Figure 6 Relation between BHN and moisture content

The BHN derived from Equation (3) and (4) was presented in Figure 6. The plot was rather scatter compared to the results obtained from 3-point flexure test. This phenomenal can be explained as *pile-up* effect. During indentation, the indentation depth imprint size increase with applied load, and plastic deformation; however, during load relaxation, elastic recovery occurs largely in the direction of the load thus affected the indentation depth measurement.

Despite that, the simplex minimization analyses revealed that proposed BHN distribution based on exponential equations still provide relatively good predictions of measured material hardness.

Due to the high dry-bonding strength characteristic of sodium bentonite, as well as the method of installation of the clay mats on sites with varying thermo-environmental and humidity level conditions, the need to understand the workable limit becomes a necessity.

On the basic of earlier experimental drying kinetic model developed by Wijeyesekera and Loh, (2005), the relative thermo-mechanical properties of the clay mat were established. In complement to these data sets, a correlation has been established in between EI and BHN as shown in Figure 7.

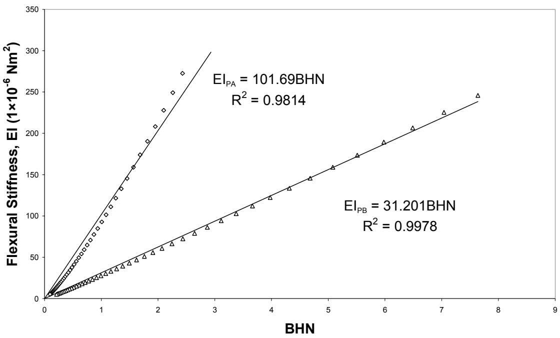

Figure 7 Correlations of EI and BHN

The EI-BHN relation can be express as follow:

$$EI_{PA} = 101.69 BHN \quad (4)$$

$$EI_{PB} = 31.201 BHN \quad (5)$$

The modified Brinell hardness test suggested in this study is more rapid and easily performed thus more practically applicable. From laboratory testing, a strong EI-BHN relationship has been developed. This relationship formed paramount information for the development of a quick assessment into the in-situ flexibility of clay mat.

4. Conclusion:

This study is the first to quantify the flexibility of saturated clay in the literature. A strong correlation between Brinell Hardness Test and 3-points bend test has been established. This provided an insight into the workable limit of clay mats in a thermal-environment condition as well as a quality control in manufacturing process. While the flexibility of clay mats is identified primarily by the change in its moisture content, it is also identified that the possibility to prolong the ductile to brittle transition of the clay mats.

5. References:

Dieter, G.E. 1988. *Mechanical Metallurgy*, McGraw-Hill, London, pp.326

McLoughlin, M. 2004. *The Influence of Mineralogy and Microstructure on the Contaminant Migration through Geosynthetic Clay Liners*. PhD Thesis, University of East London, Department of Civil Engineering, UK.

Mylvaganam, M. 2006. *The flexibility of a prehydrated bentonite with the change of its moisture content.* MSc Thesis, University of East London, Department of Civil Engineering, UK.

Wijeyesekera, D.C. and Loh, E.W.K. 2005. Mathematical Modelling of Moisture Movement in GCLs, *AC&T, SCoT 1st Annual Conference*, pp.119-123

Wijeyesekera D.C. 2003. Use and performance of bentonite in GCLs. *An International Conference on Geo-Environmental Engineering*. Keynote papers pp.27-46